The EMBO Journal Vol.18 No.23 pp.6705–6717, 1999

Kinetic dissection of fundamental processes of eukaryotic translation initiation *in vitro*

Jon R.Lorsch[1,2] and Daniel Herschlag[2]

Department of Biochemistry, Beckman Center B400, Stanford University, Stanford, CA 94305-5307, USA

[1]Present address: Department of Biophysics and Biophysical Chemistry, Johns Hopkins University School of Medicine, 725 N. Wolfe Street, Baltimore, MD 21205-2185, USA

[2]Corresponding authors
e-mail: herschla@cmgm.stanford.edu or jlorsch@jhmi.edu

Approaches have been developed for the kinetic dissection of eukaryotic translation initiation *in vitro* using rabbit reticulocyte ribosomes and a crude preparation of initiation factors. These new approaches have allowed the kinetics of formation of the 43S and 80S ribosomal complexes to be followed and have substantially improved the ability to follow formation of the first peptide bond. The results suggest the existence of a new step on the initiation pathway that appears to require at least one additional factor and the hydrolysis of GTP and may prepare the 80S complex for the formation of the first peptide bond. The initial kinetic framework and methods developed herein will allow the properties of individual species along the initiation pathway to be probed further and will facilitate dissection of the mechanistic roles of individual translation factors and their interplay with RNA structural elements.

Keywords: eukaryotic translation/GTP hydrolysis/initiation factor/kinetics/protein synthesis

Introduction

The initiation of translation in eukaryotes is an extraordinarily complex process, involving at least 24 non-ribosomal polypeptides and energy input from the hydrolysis of both ATP and GTP (Merrick and Hershey, 1996). Figure 1 shows a simplified version of the current model for eukaryotic translation initiation (Merrick and Hershey, 1996), explicitly depicting the following steps: (i) binding of methionyl initiator tRNA (Met-tRNA$_i$) and GTP to the initiation factor eIF2 to form the ternary complex; (ii) binding of the ternary complex to the 40S ribosomal subunit to form the 43S·mRNA complex (for simplicity, mRNA is shown pre-bound to the 40S subunit); (iii) joining of the 40S and 60S ribosomal subunits to form the 80S initiation complex (in this step, codon recognition, GTP hydrolysis by eIF2 and release of eIF2·GDP are omitted for clarity); (iv) binding of an aminoacyl acceptor, here puromycin, to the A-site of the ribosome; and (v) formation of the first peptide bond. While many of the initiation factors involved in this process have been identified and in some cases their basic functions have been determined, the molecular events that allow a eukaryotic ribosome to assemble on an mRNA and initiate translation remain to be elucidated (McCarthy, 1998).

To understand a process at a molecular level, a quantitative framework that describes the kinetics and thermodynamics of each step is required. Such a framework can provide insights into the functions and mechanisms of each participant in the process and serve as a foundation for more in-depth mechanistic analyses (e.g. Pollard, 1986; Stryer, 1986; Benkovic and Cameron, 1995; Gilbert *et al*., 1995; Pape *et al*., 1998). We have, therefore, set out to develop a kinetic and thermodynamic framework for eukaryotic translation initiation.

Here we describe methods for the kinetic dissection of eukaryotic translation initiation. Using these techniques, the rates of each of the steps in Figure 1 have been probed, and the results obtained suggest the existence of a new step in translation initiation involved in activating the 80S complex. The approaches and initial kinetic framework described herein should aid future mechanistic dissection of the initiation process, leading to an understanding of the molecular roles of the factors involved.

Results

The components of the system

To develop the methods needed to dissect eukaryotic translation initiation into individual steps, it was necessary to start with a system that contained all the components required for the formation of an active initiation complex. A semi-purified rabbit reticulocyte system composed of salt-washed ribosomes and a ribosomal high-salt wash fraction (HSW) containing the required initiation factors was used in these initial studies. While a fully reconstituted system (Trachsel *et al*., 1977; Benne and Hershey, 1979; Pestova *et al*., 1998) would have the advantage that the concentration of every component could be controlled independently, an analysis of the workings of a less purified system provides a useful starting point for such in-depth quantitative analyses of the individual steps that constitute this complex process. This system contains most, if not all, of the components of the translational machinery, potentially including factors that have not yet been identified. The behavior of semi-purified systems and extracts provides standards for the behavior of fully reconstituted systems and a necessary bridge between fully reconstituted and cellular systems.

The semi-purified system has also allowed us efficiently to develop assays and approaches that will be applicable to fully reconstituted systems. Furthermore, the rabbit reticulocyte system itself has been used for >20 years to study eukaryotic translation, and a quantitative analysis of its operation should aid in the interpretation of past results and the design of future experiments (e.g. Pelham and Jackson, 1976; Trachsel *et al*., 1977; Benne and

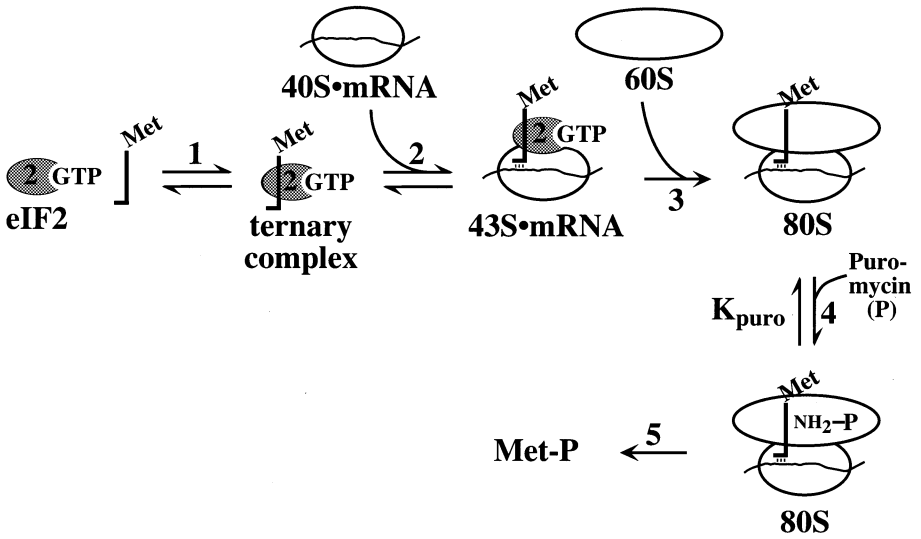

Fig. 1. Cartoon of a minimal pathway for the formation of a translation initiation complex in eukaryotes. Not all of the steps believed to be required for translation initiation are shown, and alternative pathways are possible (Merrick and Hershey, 1996). Steps involved in recognizing the 5′ cap and 3′ poly(A) tail and in scanning along an extended 5′-untranslated region (Pestova and Hellen, 1999) are omitted because a minimal RNA template lacking these features was used in this study (see Results). mRNA is shown pre-bound to the 40S subunit because saturating concentrations of the RNA template were used. Initiation factors other than eIF2 are omitted, both for simplicity and because in many cases their exact functions are not known.

Hershey, 1979; Merrick, 1979; Das *et al*., 1981; Anthony and Merrick, 1992).

A 43mer model mRNA of the sequence GGA-A(UC)$_7$UAUG(CU)$_{10}$C was used in these studies. This RNA was chosen because it is a minimal template. It is essentially poly(UC) with an AUG initiation codon in the middle so that it is expected to have no significant secondary or tertiary structure (Saenger, 1984). It also lacks the 5′ 7-methylguanosine cap, 3′ poly(A) tail and consensus sequence around the AUG codon found in natural mRNAs. The lack of these structural features simplifies the initial analysis, as steps such as cap recognition, unwinding of secondary structures and scanning for the initiation codon are not required (see Figure 1). A framework constructed with this minimal template will then allow the effects of these structural features and the factors that interact with them to be probed.

As the overall reaction, culminating in the formation of the first peptide bond, was followed using ^{35}S-labeled Met-tRNA$_i$, we ensured that this component was limiting in concentration relative to the other components. This allowed single-turnover reactions to be followed so that pre-steady-state kinetics could be investigated. Such pre-steady-state measurements are typically necessary to uncover individual reaction steps and determine their rate constants. To establish standard reaction conditions, the concentration dependencies of the components of the system were measured as described in Materials and methods and are summarized in Table I. A ribosome concentration of 0.060 μM gave maximal activity and was thus used in subsequent experiments. Titration with [^{35}S]Met-tRNA$_i$ indicated that the ribosomes could form 80S complexes and catalyze peptidyl transfer efficiently (~25% active ribosomes; Table I), in contrast to the low efficiency often observed in reconstituted systems (e.g. Hawley and Roeder, 1985; Kadonaga, 1990; Johnson and Krasnow, 1992). Finally, all small molecule components

Table I. Apparent K_ms and standard reaction conditions

Component	K_m[a] (μM)	Standard concentration (μM)
Met-tRNA$_i$	0.005[b]	0.002
GTP	3[c]	500
mRNA	<0.1	1
Puromycin (80S)	100[d]	400
Puromycin (80S*)	60[e]	400
GMP-PNP (80S)	240[f]	1000
Ribosomes	–[g]	0.06[h]

[a]Unless otherwise indicated, all apparent K_m values are for the entire initiation process starting at step 1 in Figure 1 (see Materials and methods). Values are apparent K_ms because the reactions are single turnover whereas the standard Michaelis constant is defined for multiple turnover conditions in which [enzyme]<<[substrate].
[b]This value is the mid-point of the rate of Met–Puro formation versus [Met-tRNA$_i$] plot, which is probably a titration. Thus the value is an upper limit for the apparent K_m.
[c]Values from two independent measurements were 2 and 4 μM. Experiments in which the formation of 80S* complexes from pre-formed 80S complexes was monitored following a dilution to decrease the [GTP] suggest that the apparent K_m for GTP for the conversion of 80S to 80S* is ⩽0.1 μM (data not shown).
[d]This value is the apparent K_m for reaction from the 80S complex. Two independent measurements gave values of 68 and 133 μM.
[e]This value is the apparent K_m for reaction from the 80S* complex. Two independent measurements gave values of 72 and 47 μM.
[f]Apparent K_i for GMP-PNP for inhibition of the reaction from the pre-formed 80S complex in 100 μM GTP background (33× apparent K_m). The apparent K_i is 14 μM in a background of 10 μM GTP (data not shown). Separate experiments (not shown) suggest that the inhibition is competitive with GTP. These data suggest that the relative affinities for GTP and GMP-PNP of the GTP-utilizing factors required after formation of 80S are similar.
[g]The rate of Met–Puro formation is maximal at ~0.06 μM ribosomes, but decreases at higher concentrations, presumably due to the presence of an inhibitor in the preparation. Thus 0.06 μM is unlikely to represent the true plateau of the rate of Met–Puro production and so no $K_{1/2}$ for ribosomes is given.
[h]The actual concentration of ribosomes that could form 80S complexes was estimated to be ~0.02–0.03 μM, and ~50% of the 80S complexes formed were catalytically active (unpublished observations).

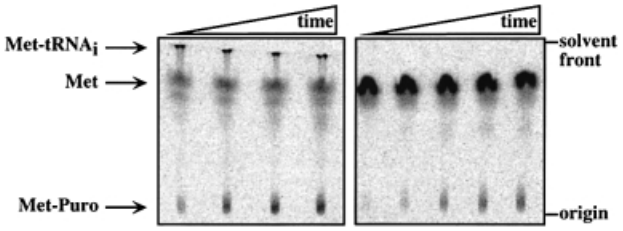

Fig. 2. Kinetics of the overall Met–puromycin formation reaction. The formation of the [^{35}S]Met–Puro dipeptide was followed using cation-exchange TLC and analyzed on a PhosphorImager. Two different time courses of the reaction are shown. Individual time points were quenched with either 3 M sodium acetate pH 4.6 (left) or 0.5 M potassium hydroxide (right). The ester linkage connecting the [^{35}S]methionine to the tRNA$_i$ is hydrolyzed by the quench in the latter case. The positions of [^{35}S]Met-tRNA$_i$, free methionine and the Met–Puro dipeptide product are indicated. At the latest time point, 15 and 5% of the total ^{35}S is present in Met–Puro for the time course on the left (15 min) and right (4 min), respectively. Time points were 2, 5, 10 and 15 min (left) and 0.5, 1, 2, 3 and 4 min (right). The smear below the free methionine may be oxidized methionine. Details of the assay are given in Materials and methods.

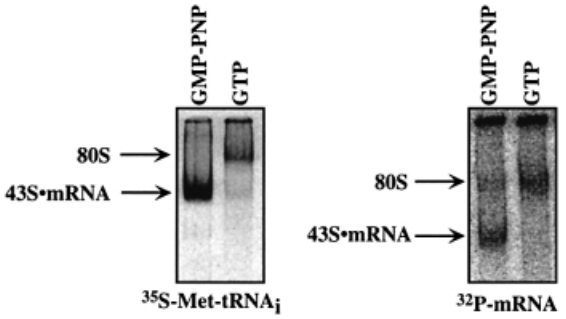

Fig. 3. Native gel assay for the formation of 43S·mRNA and 80S complexes. The 43S complexes were formed in the presence of GMP-PNP, which blocks the reaction prior to subunit joining (Figure 1, step 3; e.g. Trachsel, 1996), and 80S complexes were formed in the presence of GTP, which allows subunit joining to take place. Reactions were resolved on 4% polyacrylamide gels in 1× THEM as described in Materials and methods and analyzed on a PhosphorImager. The positions of the complexes were followed using either [^{35}S]Met-tRNA$_i$ (left) or ^{32}P-labeled mRNA (right). The gel on the right was run for longer, resulting in the better separation. The material at the top of the gel may be RNA–protein aggregates, as discussed in Materials and methods. The smaller amount of 80S complex formed relative to the amount of 43S·mRNA complex formed (compare GMP-PNP and GTP lanes in the left panel) presumably is due to a fraction of inactive 43S·mRNA complexes that cannot go on to form 80S complexes (~50%; Table I).

of the system and the model mRNA were saturating under the standard assay conditions (Table I).

Assays for the kinetic dissection of translation initiation

The standard assay for following the formation of an active translation initiation complex is the puromycin assay. In this assay, a [^{35}S]methionine-charged initiator tRNA (Met-tRNA$_i$) is bound in the P-site of the 80S ribosomal complex. The drug puromycin, an analog of the 3′ end of a charged tRNA, can bind in the A-site of the ribosome, and the ribosome can catalyze the attack of the amine of puromycin on the ester linkage of Met-tRNA$_i$ to form a [^{35}S]methionine–puromycin dipeptide (Met–Puro). This assay reflects all the steps shown in Figure 1, including the formation of the first peptide bond.

Traditionally, reaction mixtures have been extracted with ethyl acetate, which specifically removes the [^{35}S]Met–Puro product but not the [^{35}S]Met-tRNA$_i$ or free [^{35}S]methionine from the aqueous reaction mixture (Leder and Bursztyn, 1966; Merrick, 1979). The amount of [^{35}S]Met–Puro in this organic phase is then determined by scintillation counting. We have developed a cation-exchange thin-layer chromatography (TLC) method that reduces the amount of material required for the assays by over an order of magnitude relative to the standard ethyl acetate extraction procedure (1–2 µl versus 25–50 µl reaction volumes per time point, respectively; e.g. Merrick, 1979; see Materials and methods). Furthermore, unlike the ethyl acetate extraction procedure in which only the dipeptide product is observed, the TLC analysis allows direct observation of the Met-tRNA$_i$, Met–Puro and free methionine (Figure 2). Finally, because the ratio of product formed to starting material can be taken for each time point, inaccuracies from pipeting are diminished, and, because free methionine is also observed, the hydrolysis reaction can be monitored directly and the presence of free methionine accounted for.

To dissect the initiation process into individual steps, it is also necessary to have assays to follow the formation of reaction intermediates such as the 43S·mRNA complex and the 80S complex. While these complexes can be separated by sucrose gradient sedimentation experiments, this procedure is not amenable to kinetic analysis because the number of samples that can be processed per experiment is small. Furthermore, during the ultracentrifugation and fractionation steps, it is not possible to stop the reactions from continuing or prevent the complexes from dissociating. Glutaraldehyde has been used in the past to attempt to cross-link the complexes together and stop the reactions from proceeding further. This procedure, however, disrupts the 43S·mRNA complex and may also alter the amount of 80S complex present (Chatterjee *et al*., 1979; data not shown).

Native gels have been used in the past to separate prokaryotic ribosomal subunits (Dahlberg, 1979) and frequently are used in analysis of spliceosome formation (e.g. Konarska and Sharp, 1986; Cheng and Abelson, 1987; Seraphin and Rosbash, 1989). Upon entering the gel matrix, the protein–nucleic acid complexes are often trapped and cannot dissociate or react further. This caging phenomenon is the basis for the standard gel mobility shift assay (Vossen and Fried, 1997). We reasoned that the same approach might work for the kinetic analysis of 43S·mRNA and 80S complex formation. As shown in Figure 3 and described in Materials and methods, 43S·mRNA complexes can be separated from 80S complexes on 4% polyacrylamide native gels. The complexes can be labeled with either [^{35}S]Met-tRNA$_i$ or [^{32}P]mRNA and the reactions can be stopped at the 43S·mRNA complex stage by substituting the slowly hydrolyzable GTP analog GMP-PNP for GTP, as expected because GTP hydrolysis is required for step 3 (Figure 1; e.g. Trachsel, 1996). By directly loading aliquots from a reaction on a running native gel, time points as early as 30 s can be resolved.

Details of these techniques and of the identification of

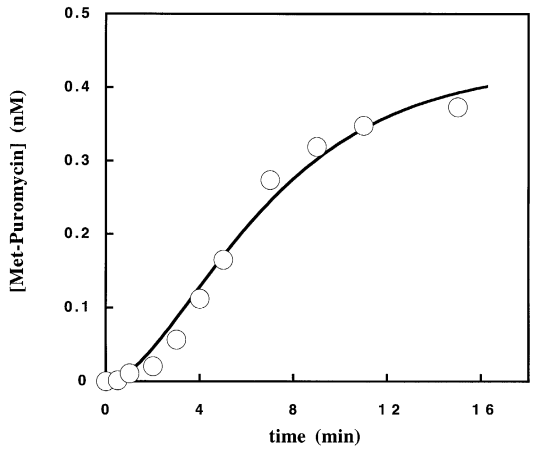

Fig. 4. A lag phase in the formation of Met–Puro. A time course of Met–Puro formation is shown. Reactions were initiated by the addition of ribosomes and high-salt wash, and the formation of [^{35}S]Met–Puro was followed by analyzing individual time points using the TLC assay (see Materials and methods). The curve is the best fit of the data by the equation describing a simple two-step process (see Materials and methods). The observed first-order rate constants for the first and second steps from this fit are each 0.3/min. The range of values for these rate constants from five independent experiments was 0.2–0.4/min.

the reactants and products in the TLC system and of the ribosomal complexes in the native gel system are described in Materials and methods.

Kinetics of translation initiation in vitro

A lag phase in the formation of Met–Puro dipeptide. The kinetics of the overall reaction, starting at step 1 and proceeding all the way to peptide bond formation to give [^{35}S]Met–Puro (Figure 1), was followed using the TLC assay and the standard single-turnover conditions described above (Table I). As shown in Figure 4, there is a distinct lag phase in the formation of Met–Puro. The lag phase indicates that there are at least two slow steps with similar observed rate constants on the pathway to Met–Puro formation. The data are fit well by the equation describing an irreversible two step process (see Materials and methods) in which the reactants must first form an intermediate before the Met–Puro product can be formed and in which each step occurs with apparent first-order rate constants, k_{obs}, of ~0.3/min. Deviations of this fit from the experimental data could be due to small contributions to the overall rate equation from other steps on the pathway, to some reversibility of the steps or to experimental error.

Kinetic dissection to identify the slow steps on the initiation pathway. To determine which steps along the initiation pathway shown in Figure 1 are the slow steps in this system, the observed rate constants for the formation of the 43S·mRNA complex and the 80S complex were determined. The reaction was either blocked at the 43S·mRNA complex stage by including GMP-PNP instead of GTP in the reaction or allowed to go on to form the 80S complex with the normal GTP cofactor. Time points from these reactions were analyzed on native gels as described above ('Assays for the kinetic dissection of translation initiation'). The experiments described below

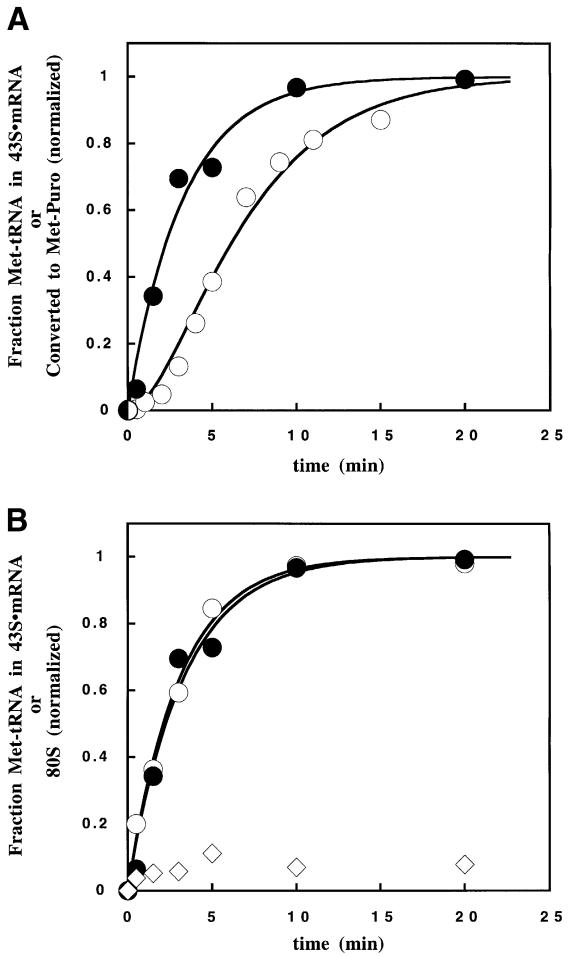

Fig. 5. Formation of the 43S·mRNA complex accounts for the lag phase in Met–Puro production and the 60S subunit joining step is fast. (**A**) A time course for 43S·mRNA formation (●) compared with the formation of Met–Puro (○; from Figure 4). The formation of 43S·mRNA complex in the presence of 1 mM GMP-PNP was followed using [^{35}S]Met-tRNA$_i$ and the native gel assay described in Materials and methods. The data are normalized to the end point of each reaction (the ratio of [Met–Puro]/[43S·mRNA] at the end points is ~0.5). The curve is the best fit of the data by a single exponential equation describing a first-order process with k_{obs} = 0.3/min. The rate constants from two other, independent experiments (not shown) were 0.3 and 0.4/min. (**B**) Comparison of 43S·mRNA complex formation (●) in the presence of 1 mM GMP-PNP and 80S (○) and 43S·mRNA (◇) formation in the presence of 0.5 mM GTP. The reactions were followed as in (A). The data are normalized to the end point of each reaction [43S·mRNA complex formation in the presence of GTP was normalized to the end point of 80S formation; the ratio of 43S·mRNA (GMP-PNP)/80S (GTP) end points is 1.4]. The curves are the best fits of the data by a single exponential equation for a first-order process; k_{obs} for 43S·mRNA and 80S complex formation are both 0.3/min, indicating that the subunit joining step is fast relative to the formation of 43S·mRNA complex (>1/min). The same result was obtained in two other, independent experiments. The kinetics of formation of both 43S and 80S complexes are monophasic, suggesting that the ribosomes that are capable of forming these complexes behave as single populations in these two steps.

are, to our knowledge, the first measurements of the rates of formation of eukaryotic ribosomal complexes.

A comparison of the kinetics of 43S·mRNA formation and the formation of Met–Puro in the overall reaction is shown in Figure 5A. Formation of 43S·mRNA (closed circles) takes place largely during the lag phase of

the overall Met–Puro formation reaction (open circles). Furthermore, the observed rate constant for 43S·mRNA complex formation obtained from the first-order fit to the data in Figure 5A is 0.3/min, the same as the rate constant for the first slow step in the overall Met–Puro formation reaction (Figure 4). These data suggest that the first slow step occurs in the pathway leading to the formation of the 43S·mRNA complex (Figure 1, steps 1 or 2) and that the second slow step occurs after this complex has been formed.

The kinetics of 43S·mRNA complex formation in the presence of GMP-PNP was next compared with the kinetics of 43S·mRNA and 80S complex formation in the presence of GTP (Figure 5B). The time course of 43S·mRNA formation with GMP-PNP is indistinguishable from that of 80S formation with GTP (Figure 5B; closed and open circles). Furthermore, in the presence of GTP, little 43S·mRNA complex builds up during the reaction (Figure 5B, diamonds). Thus, under these conditions, the steps required for 60S subunit joining (Figure 1, step 3) are fast relative to the formation of 43S·mRNA complex and to the second slow step in the pathway.

These results also indicate that the second slow step on the pathway occurs after 80S complex formation and thus involves either puromycin binding or peptide bond formation (Figure 1, step 4 or 5). The nature of this step is addressed below, after describing further characterization of the first slow step.

Is the formation of the ternary complex or the 43S·mRNA complex the first slow step? To determine whether the formation of the ternary complex (Figure 1, step 1) or the 43S·mRNA complex (Figure1, step 2) is the first slow step on the pathway, the relative rates of formation of these two species were probed. This was accomplished by pre-incubating the HSW containing the initiation factors with GTP and [^{35}S]Met-tRNA$_i$ in the absence of ribosomes for 3–10 min to allow time for the ternary complex to form (step 1). Ribosomes, mRNA and puromycin were then added. If ternary complex formation (step 1) were the slow step, then the reaction would now have no lag phase and would be predicted to proceed with a single rate constant of 0.3/min, corresponding to the second slow step on the initiation pathway. In contrast, if the formation of the ternary complex were fast and formation of the 43S·mRNA complex were the first slow step in the pathway, then pre-forming the ternary complex would have no effect on the kinetics of the overall reaction as two slow steps would remain before Met–Puro production (Figure 1, step 2 and e.g. step 5).

The time course of Met–Puro formation following a pre-incubation is shown in Figure 6A. The reaction now follows a single rate constant without a lag phase. Furthermore, the observed first-order rate constant of 0.3–0.6/min (range of values from three independent experiments) is consistent with the value of ~0.3/min obtained independently for the second slow step on the pathway under the standard reaction conditions (Figure 4). These results suggest that the formation of the ternary complex (step 1) is the first slow step on the overall initiation pathway.

Further evidence that ternary complex formation is the first slow step was provided by monitoring the formation of the 43S·mRNA complex directly on a native gel. Pre-incubation in the absence of ribosomes was performed to allow formation of the ternary complex, as described above, but with GMP-PNP substituted for GTP to block the reaction at the 43S·mRNA complex stage. The reaction was initiated by the addition of ribosomes, and time points from the reaction were analyzed by native gel. The formation of 43S·mRNA complexes was complete by 30 s, the first time point (data not shown), whereas only ~10% of this complex was formed in 30 s without the pre-incubation (Figure 5A). The rapid formation of the 43S·mRNA complex following the pre-incubation indicates that this complex forms with a rate constant of

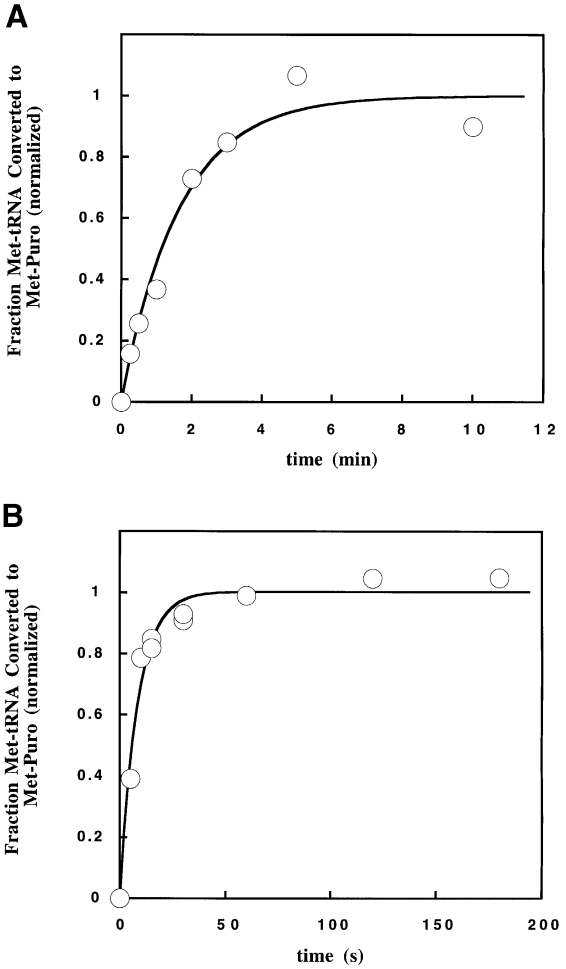

Fig. 6. Pre-incubations allow further dissection of the pathway. (**A**) Pre-incubation of HSW, [^{35}S-Met]tRNA$_i$ and GTP for 3 min prior to initiating the reaction by adding ribosomes and puromycin eliminates the lag phase in Met–Puro formation. The data from the time course of Met–Puro formation are well fit by a single exponential equation with k_{obs} = 0.6/min (solid line). Values for k_{obs} from two other, independent experiments were 0.3 and 0.6/min. (**B**) Pre-incubation of all of the reaction components except puromycin leads to a 30-fold activation of the 80S complex. Reaction components were incubated for 10 min in the absence of puromycin and the reaction was then initiated by addition of puromycin and the formation of Met–Puro was monitored. A first-order fit of the data yielded a value of k_{obs} of 7/min. Three other, independent experiments (Figure 8B; not shown) gave values of k_{obs} of 9–11/min. No increase in activity was seen if the HSW was absent from the pre-incubation. Note that the time scale in (B) is seconds.

>3/min under the standard reaction conditions (Figure 1, step 2), at least an order of magnitude faster than the slow steps.

Additional experiments demonstrated that the elimination of the lag phase requires the presence of Met-tRNA$_i$ during the pre-incubation (data not shown). This suggests that the slow step is on the pathway to eIF2·GTP·Met-tRNA$_i$ complex formation and is not a process that does not involve eIF2·Met-tRNA$_i$ such as the assembly of an initiation factor complex. The slow step could be a first-order process, such as a conformational change in eIF2, a higher order process, such as binding of Met-tRNA$_i$ to eIF2, or the release of bound GDP from eIF2 (Trachsel, 1996).

The length of the lag phase of the reaction is dependent on the concentration of HSW (data not shown), suggesting that the slow step is second or higher order. Furthermore, the rate of forming the intermediate complex that follows the first slow step increases with increasing Met-tRNA$_i$ concentration, also suggesting that the first slow step involves more than eIF2 alone. These and other observations from this semi-purified system will guide future experiments with purified eIF2 to determine the nature of this step and will allow results from such experiments to be integrated into the overall framework for translation initiation.

Activation of the 80S complex. The above results predict that if the reactions were started at the 80S complex stage, there would be no lag phase in the formation of Met–Puro and that the formation of Met–Puro would proceed with a rate constant of ~0.3/min. To test this, all the components of the reaction except puromycin were pre-incubated for 10 min. This incubation allows sufficient time for the complete formation of 80S complexes, given the observed rate constant of ~0.3/min for the process. The reactions were then initiated by adding puromycin, and the formation of Met–Puro was monitored (Figure 6B). As predicted, the lag phase in Met–Puro formation is eliminated by the pre-incubation. However, rather than proceeding with an observed rate constant of 0.3/min, the reaction was ~30-fold faster, with $k_{obs} \approx 10$/min. These data are fully consistent with the above assignment of ternary complex formation as the first slow step, but require the addition of a new step to the minimal mechanism of Figure 1. This new step is a 30-fold activation of the 80S complex. This activated state will be referred to hereafter as the 80S* complex. Experiments described in the following sections were designed to probe its formation and properties.

Probing the architecture of the initiation pathway. We first considered whether the pathway for formation of an active initiation complex is linear or branched. In the linear pathway model, the conversion of 80S to 80S* must occur before puromycin can bind productively to the ribosome (Scheme 1A). The rate constant for this conversion step, the second slow step in the reaction which limits the rate of formation of Met–Puro, would then be 0.3/min. If this slow step is passed by pre-incubating the components of the reaction in the absence of puromycin, the rate-limiting step would become formation of Met–Puro from the 80S* complex, and the reaction would proceed with an observed rate constant of 10/min. In contrast, in the branched pathway model of Scheme 1B, puromycin could react with either the 80S complex, to produce Met–Puro with a k_{obs} of 0.3/min, or with the 80S* complex, to produce Met–Puro with a k_{obs} of 10/min (Scheme 1B and Figure 7, bottom).

Scheme 1A

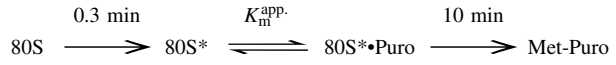

Scheme 1B

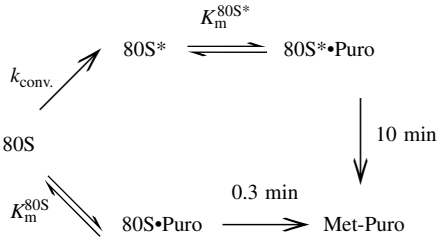

A specific prediction of the linear model (Scheme 1A) is that the apparent K_m for puromycin for reaction from the 80S complex should be ~30-fold lower than the apparent K_m for reaction from the 80S* complex (i.e. $K_m^{80S} = 1/30 \times K_m^{80S*}$). This can be explained as follows. The rate of reaction would only increase with increasing puromycin concentration until an observed first-order rate constant for the reaction from 80S* of 0.3/min was achieved. It would not increase beyond 0.3/min with further increases in the puromycin concentration despite the maximal rate of 10/min for Met–Puro formation from 80S* because the rate of the reaction would be limited by the rate of conversion of 80S to 80S* (Scheme 1A). This change in rate-limiting step would cause K_m^{80S}, which represents the puromycin concentration that gives the half-maximal rate of peptide bond formation in the overall reaction, to be 30-fold below the concentration for half-maximal peptide bond formation starting from 80S*, K_m^{80S*}. The value of 30 arises because the maximal rate for the reaction starting from 80S of 0.3/min is 30-fold less than the value of 10/min starting from 80S* (Fersht, 1985; Jencks, 1987). In contrast, although more complex scenarios are possible, the branched pathway would allow the apparent K_m values for reactions starting from the 80S and the 80S* complexes to be the same (Scheme 1B and Figure 7).

We therefore determined the observed puromycin K_m values for reactions starting from the 80S complex and from the 80S* complex. The similar values of $K_m^{80S} = 100$ μM and $K_m^{80S*} = 60$ μM (Table I) are consistent with the branched model shown in Scheme 1B, but are inconsistent with the 30-fold difference predicted by the linear model. These results, combined with those presented below, lead to the working model presented in Figure 7, although other branched pathways are also possible.

To characterize the initiation pathway further, the rate constant for the conversion of 80S to 80S* was determined (Scheme 2). Because Met–Puro is formed 30-fold faster

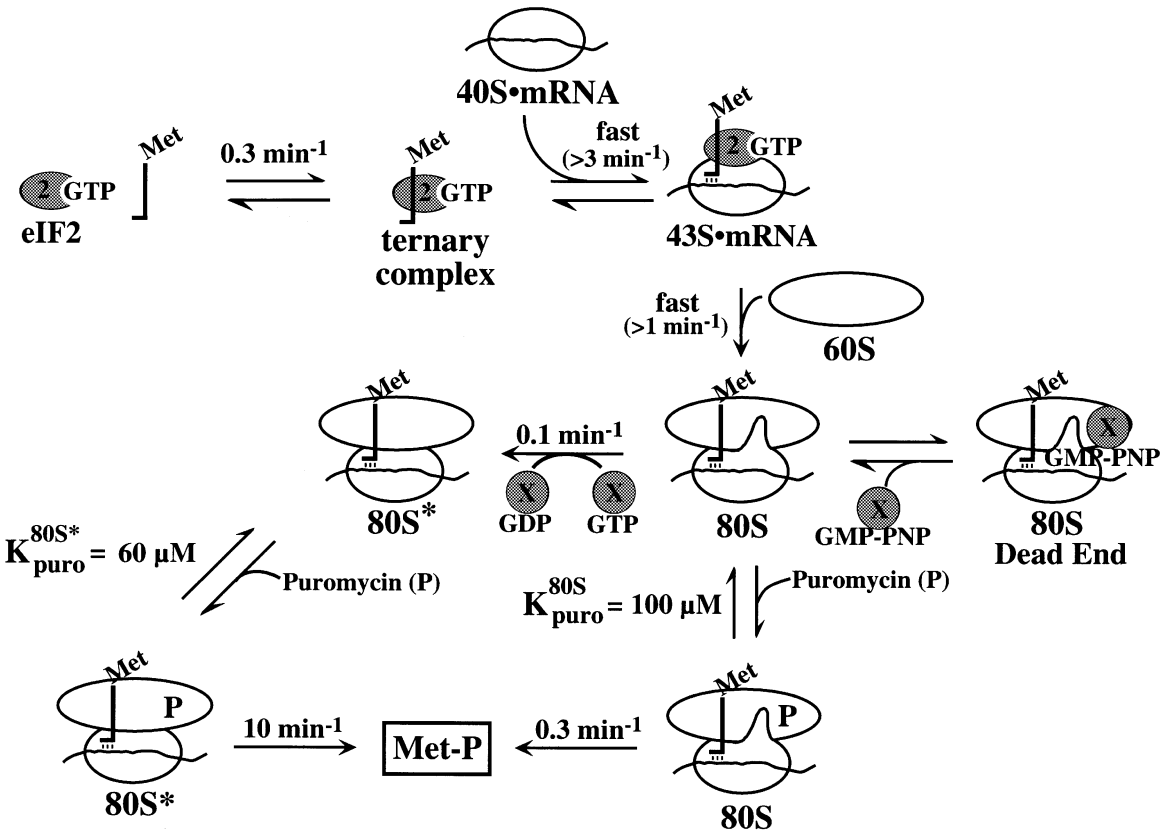

Fig. 7. Kinetic framework for translation initiation in the rabbit reticulocyte system summarizing the data presented in this work. The data suggest that formation of the ternary complex is the slow step preceding peptide bond formation under the conditions used. Binding of the ternary complex to the 40S·mRNA complex and joining of the 60S subunit to the 40S subunit to form the 80S complex (several steps; Figure 1 legend) are both fast relative to formation of the ternary complex, formation of Met–Puro from the 80S·puromycin complex and conversion of 80S to 80S*. The 80S to 80S* conversion step may be a conformational rearrangement of the 80S complex, shown schematically as the disappearance of a protrusion on the 40S subunit. GMP-PNP inhibition (Figure 8) and dilution chase experiments (Figure 9) suggest the existence of at least one additional factor ('Factor X' circle) that uses the energy from GTP hydrolysis to catalyze the transformation of 80S to 80S*. A postulated complex with Factor X·GMP-PNP bound to the 80S ribosome can account for the observed inhibition of reaction from 80S by GMP-PNP ('Dead End'), although other models are also possible. K_{puro}^{80S} and K_{puro}^{80S*} are the apparent Michaelis constants for puromycin reaction from the 80S and 80S* complexes, respectively (see Results and Table I). All rate constants shown are observed first-order rate constants under the conditions of this system and do not imply the molecularity of the processes.

from 80S* than from 80S, the amount of 80S* present at a given time can be measured by the amount of Met–Puro that is formed rapidly following addition of puromycin. Thus, the conversion of 80S to 80S* can be followed by adding puromycin after incubating the 80S complex for varying times (Scheme 2, t_1). A rate constant for this conversion of 0.1/min was obtained in two independent experiments (data not shown; Figure 7). Although this rate constant is only 3-fold smaller than the rate constant of 0.3/min for Met–Puro formation from the 80S complex, it should be noted that the linear pathway model (Scheme 1A) predicts that the rate constant for conversion of 80S to 80S* should be ≥0.3/min.

Scheme 2

$$\xrightarrow{t_1\ \text{Puromycin}}$$

$$80S \rightarrow 80S \;+\; 80S^* \rightarrow \text{Assay}$$

The conversion of 80S to 80S is inhibited by GMP-PNP.* To probe the two pathways for formation of Met–Puro shown in Figure 7 (bottom), the sensitivity of each of these pathways to inhibition by GMP-PNP was investigated. GMP-PNP is a slowly hydrolyzable GTP analog that can block many processes involving GTP (e.g. Yount, 1975; Nissen *et al.*, 1996). The GMP-PNP sensitivity of the reaction starting at the 80S complex was first investigated. The 80S complex was formed by pre-incubating the reaction components in the absence of puromycin for 3 min. Reactions were then initiated by adding puromycin (Figure 8A, solid triangles) or puromycin plus saturating GMP-PNP (1 mM; open circles), and Met–Puro formation was monitored. GMP-PNP severely inhibits the formation of Met–Puro when the reactions are started at the 80S complex stage (compare solid triangles with open circles in Figure 8A). The burst of ~25% Met–Puro formation is accounted for by the formation of some 80S* during the 3 min pre-incubation used to form 80S complexes and the absence of inhibition of Met–Puro formation from the 80S* complex (see below). In contrast to the inhibition observed with GMP-PNP, the same concentration of AMP-PNP had no effect on the reaction from the 80S complex (data not shown). Varying the concentration of GMP-PNP in the reaction yielded an apparent K_i of 240 µM for inhibition by GMP-PNP in the presence of 100 µM GTP and of 14 µM in the presence of 10 µM GTP (data not shown; see Table I and Materials

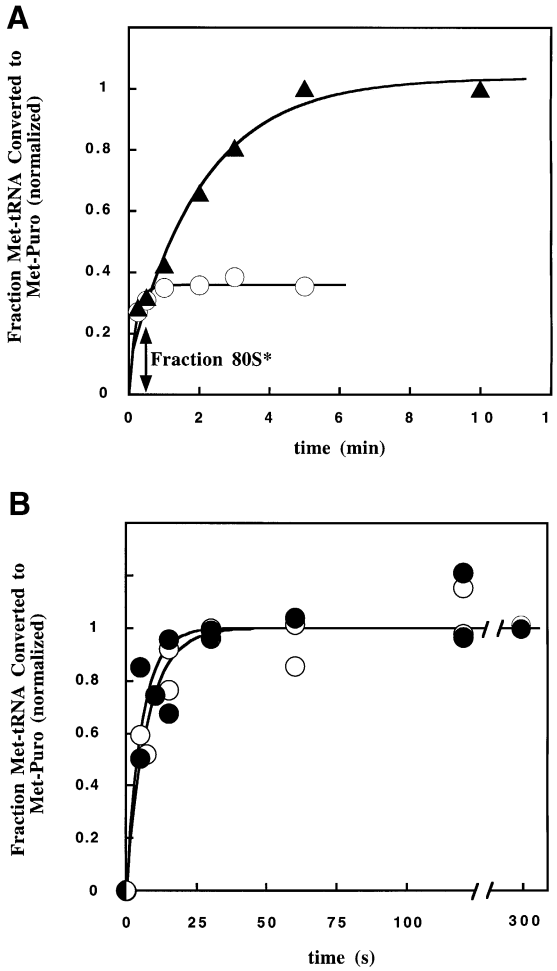

Fig. 8. GMP-PNP inhibits reaction from 80S but not from 80S*. (**A**) Reaction from 80S is inhibited by GMP-PNP. Ribosomes, HSW, [^{35}S]Met-tRNA$_i$ and 100 μM GTP were pre-incubated for 3 min to allow formation of the 80S complex. The reaction was then initiated by adding puromycin (▲) or puromycin plus 1 mM GMP-PNP (○) and the formation of Met–Puro was followed. During the pre-incubation, a small fraction of the 80S complex (~25%) goes on to form 80S*. This fraction is reflected in the small burst in Met–Puro formation in both cases (double-headed arrow). The data were fit by a double exponential equation describing two first-order processes (no GMP-PNP; ▲) or a single exponential (GMP-PNP; ○) and were normalized to the end point in the absence of GMP-PNP. The rate constant for the first (fast) phase was set at 10/min for the double exponential fit (Figure 6B). The best fit value for k_{obs} (slow phase) in the absence of GMP-PNP (▲) was 0.5/min. (**B**) GMP-PNP does not inhibit reaction from the 80S* complex. As in (A), except that the reactions were pre-incubated for 10 min prior to initiating the reactions by addition of puromycin (○) or puromycin plus 1 mM GMP-PNP (●). The 10 min pre-incubation was sufficient to allow near complete formation of 80S*. The data are normalized to the end point of each reaction (end points were the same in the presence and absence of GMP-PNP). Fitting the data with first-order equations yielded observed rate constants of 8 and 10/min in the absence and presence of GMP-PNP, respectively. The same result was obtained if, after the first 10 min pre-incubation to form 80S*, the reaction was incubated for an additional 10 min with 1 mM GMP-PNP and then initiated by adding puromycin (not shown).

and methods). These data suggest the existence of a step or steps after the formation of the 80S complex that requires GTP hydrolysis.

Severe inhibition of Met–Puro production was also observed if the 80S complexes were pre-formed and then incubated for 10 min in the presence of 1 mM GMP-PNP, with puromycin added after this incubation (data not shown). In the absence of GMP-PNP, the 10 min incubation is sufficient for nearly all of the 80S complexes to go on to form 80S* complexes (k_{obs} = 0.1/min; see above). The inhibition in this experiment suggests that, in addition to inhibiting production of Met–Puro by the 80S complex, GMP-PNP inhibits either the conversion of 80S to 80S* or production of Met–Puro by 80S* itself.

To differentiate between these possibilities, the sensitivity to GMP-PNP of the reaction from the 80S* complex was tested (Figure 8B). The 80S* complex was formed during a 10 min pre-incubation of all the reaction components in the absence of puromycin. The reactions were then initiated by addition of puromycin or puromycin plus 1 mM GMP-PNP. As seen in Figure 8B, there is no inhibition of reaction from the 80S* complex by GMP-PNP. In addition, 80S* complexes that were formed as described above were incubated for 10 min with 1 mM GMP-PNP prior to initiation of the reaction with puromycin. GMP-PNP again had no effect on the reaction from the 80S* complex (data not shown). Thus, reaction from the 80S* complex is not inhibited by GMP-PNP. Combined with the above results, the data strongly suggest that the conversion of the 80S to the 80S* complex is inhibited by GMP-PNP.

A factor in the high-salt wash is involved in the 80S to 80S conversion.* If a soluble factor in the HSW were required for the conversion of the 80S complex to the 80S* complex, dilution of the HSW might slow this transformation by lowering the concentration of the required factor. To test this possibility, the 80S complex was formed as described above. The 80S complexes and the HSW were then diluted 5-fold in reaction buffer. The concentration of GTP was kept constant before and after dilution. The diluted reaction was incubated for 10 min, a time that is sufficient for 80S* formation in the undiluted case (Figure 9, open circles), and puromycin was then added to allow peptide bond formation. In the diluted reaction, a fraction of the ribosomes had formed the 80S* complex during the incubation to form 80S, giving the observed ~30% burst of Met–Puro formation, as seen in experiments described earlier (Figure 8A). The majority of the ribosomal complexes in the diluted reaction, however, reacted with puromycin to form Met–Puro with an observed first-order rate constant of 0.3–0.6/min (Figure 9; data not shown). This is ~30-fold slower than reaction from the 80S* complex. In contrast, analogous dilution subsequent to formation of the 80S* complex had no effect on the rate of Met–Puro formation upon addition of puromycin (data not shown). These data thus suggest that the 5-fold dilution of the HSW and ribosomes significantly slows the conversion of 80S to 80S*.

The above experiments suggest that at least one factor in the HSW is involved in converting the 80S complex into the 80S* complex. It is possible that this factor is an integral ribosomal protein that is lost during the high-salt wash step (see Materials and methods) and that rebinding of this protein is responsible for the activation. If this were the case, then incubation of ribosomes and HSW prior to addition of the other components of the reaction might have been expected to result in formation of 80S* complexes directly upon 60S joining. However, such

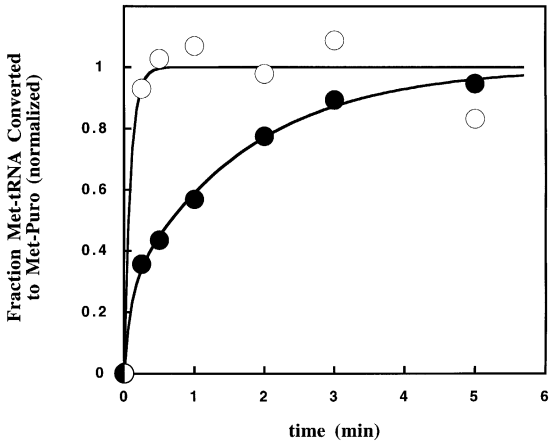

Fig. 9. The transformation of 80S to 80S* is slowed by dilution of the HSW relative to the ribosomes. 80S complexes were formed as in Figure 8A and reactions were then either diluted 5-fold in reaction buffer plus 0.5 mM GTP (●) or not diluted (○) and incubated for 10 min to allow time for 80S to be converted to 80S*. The reactions were initiated by the addition of puromycin and the formation of Met–Puro was monitored. The data for the dilution experiment were fit with a double exponential (●) and the data without dilution were fit with a single exponential (○), as described in Figure 8. The fit to the 5-fold dilution data gave a k_{obs} value of 0.6/min for the second (slow) phase, consistent with reaction from the 80S complex. In four other, independent experiments, k_{obs} ranged from 0.3 to 0.6/min (not shown). The fit to the undiluted data gave a k_{obs} value of 11/min, as expected for reaction from 80S*. Dilution of the 80S complexes 5-fold while holding the concentration of HSW constant had no effect on the conversion of 80S to 80S* (data not shown), indicating that ribosome–ribosome interactions are not responsible for the concentration dependence of the conversion step.

pre-incubation did not increase the activity of the 80S complexes initially formed, and these complexes still required further incubation for activation to the 80S* state (data not shown). In addition, literature results suggest that the monovalent salt concentration used in the preparation of the ribosomes (0.5 M) does not dissociate ribosomal proteins from mammalian ribosomal subunits (Cox *et al*., 1976; Nesset and Dickman, 1980). Finally, the apparent requirement for GTP hydrolysis suggests a more active event than simply the rebinding of an integral ribosomal protein (see Discussion).

Probing the role of mRNA structural elements. Because a tight binding, unstructured model mRNA was used in this system, steps involved in binding of the mRNA to the ribosome (e.g. cap recognition, 43S binding to the mRNA and scanning) are unlikely to be revealed by the kinetics of the reactions described. The unstructured model mRNA was used to simplify the initial analysis and to lay the foundation for future studies to probe the role of structural elements in the mRNA such as the 5′ cap, 3′ poly(A) tail, secondary and tertiary structures and the consensus sequence around the AUG codon. Comparisons of the kinetic framework made with the minimal model mRNA and frameworks made using model mRNAs with each structural element will allow the effects of mRNA structures on each step in the initiation pathway to be determined.

As a starting point for such studies, the effect of a 5′ cap on the kinetics of the Met–Puro formation reaction was probed. The presence of a 5′ cap on the model mRNA has no effect on the kinetics of either of the slow steps of the reaction with 1 or 0.1 μM model mRNA (k_{obs} = 0.3/min for both steps; data not shown). The cap structure probably increases the affinity of the 43S complex for the mRNA via interactions with the eIF4F complex and other initiation factors. However, this step is already rapid in this system, presumably because the model RNA is unstructured and present at saturating concentrations. The presence of 0.8 mM cap analog (7-MeGpppG), a concentration well above the K_d for eIF4E (Wieczorek *et al*., 1998), has no effect on the kinetics of the overall reaction (data not shown), consistent with fast, strong binding of the model mRNA that does not require a 5′ cap for increased affinity. It was also found that the 80S activation step occurs with a capped model mRNA, suggesting that this step is not specific to uncapped messages (data not shown). It will be necessary in future experiments to unravel the RNA features, initiation factors and other proteins necessary to recapitulate the cap dependence observed *in vivo* and then to dissect the steps affected (e.g. Tarun and Sachs, 1995; Merrick and Hershey, 1996; Svitkin *et al*., 1996).

Discussion

We have described new methods that allow individual steps in eukaryotic translation initiation to be probed kinetically. The results provide an initial kinetic framework for this complex process, which includes a new GTP-dependent step late in the initiation pathway, as summarized in Figure 7 and discussed below. Further application of the approaches described herein, in conjunction with current research into the roles and structures of the initiation factors (e.g. Marcotrigiano *et al*., 1997; Matsuo *et al*., 1997; Pestova *et al*., 1998), should allow still deeper mechanistic dissection of the initiation pathway, its individual steps and the roles of individual factors and RNA elements in these steps. To understand this complex biological process fully, it will also be necessary to relate the behavior of crude extracts and partially purified systems to *in vivo* behavior and to the properties of systems reconstituted from purified components. The system used in this work represents an intermediate between *in vivo* studies and studies using fully reconstituted systems, as the crude preparation of translational components used contains both known and potentially unknown factors, while still allowing significant control over the concentrations and structures of the components.

Probing individual steps in translation initiation in vitro

We have followed translation initiation using partially purified ribosomes and initiation factors from rabbit reticulocytes, with limiting ^{35}S-labeled Met-tRNA$_i$ and saturating model mRNA, GTP and puromycin. The data suggest that under these conditions, formation of the eIF2·GTP·Met-tRNA$_i$ ternary complex is one of two slow steps for formation of the first peptide bond and is responsible for the observed lag phase. Formation of the ternary complex, itself a complicated process, is limited by a step that requires Met-tRNA$_i$ and initiation factors but not GTP (data not shown). Filter binding assays using purified eIF2 (Chatterjee *et al*., 1979) and the native gel

assay for 43S complex formation described herein should allow future dissection of this process.

Binding of the ternary complex to the 43S·mRNA complex and the subsequent steps required for 60S subunit joining to form the 80S complex are at least an order of magnitude faster than ternary complex formation (Figure 7). These steps contribute little to the overall rate of formation of a translation initiation complex in this system and will require further fractionation to probe it directly.

The second slow step under these conditions occurs subsequent to the formation of the 80S complex. As puromycin was saturating in these experiments, the simplest model is that this step is the actual formation of the peptide bond. Nevertheless, the results discussed in the following section suggest that the processes occurring subsequent to 80S complex formation are more complex than previously recognized.

The observed rate constants of ~0.3/min for the two slow steps are ~30-fold slower than *in vivo* estimates for translation initiation (Palmiter, 1975). Although the observed activation of the 80S complex increases the second of these rate constants to 10/min, a process can occur no faster than the slowest step. The simplest explanation for this difference is that one or more initiation factors involved in ternary complex formation, the first slow step, are present at higher concentration *in vivo*. Our HSW preparation only includes those factors stably associated with the ribosomes prior to the high-salt wash step. It also remains possible that one or more factors are absent. The initial framework established herein and the ability to follow individual steps of translation initiation should allow identification of such factors.

It is likely that the kinetics of translation initiation *in vivo* on a natural mRNA will be different from those reported in this *in vitro* system using a minimal model mRNA. *In vivo*, with long, highly structured mRNAs, cap recognition, binding of the mRNA to the 43S complex and scanning for the AUG codon are all thought to be important steps in the rate of formation of an initiation complex (Jackson, 1996), whereas these steps are not observed in this system (see also 'Probing the role of mRNA structural elements' in Results). Furthermore, the rate of translation of an mRNA *in vivo* could be set by elongation or termination events, steps not explored in this work.

A new step in eukaryotic translation initiation?

In the course of this kinetic analysis, evidence unexpectedly was uncovered for a new step in initiation. This step results in the 30-fold activation of the 80S complex to produce a new complex which we have called 80S* (Figure 7). Activation is inhibited by GMP-PNP (Figure 7, '80S, Dead End'), and dilution experiments suggest the involvement of at least one HSW factor (Figure 7, 'X'). Figure 7 depicts the simplest model to explain these data in which a GTPase helps to catalyze the conversion of the 80S complex to the 80S* complex. It is possible that the GMP-PNP inhibition of Met–Puro formation from the 80S complex reflects the action of this or another GTPase in this route to peptide bond formation as well.

The conversion of 80S to 80S* may be a conformational reorganization that requires the energy from GTP hydrolysis. This proposal is shown schematically in Figure 7 as the disappearance of a protrusion on the 40S subunit. This conformational reorganization could be similar to the EF-G·GTP-catalyzed reorganization of the prokaryotic ribosome that is required after the formation of each peptide bond during elongation (Abel and Jurnak, 1996; Rodnina *et al*., 1997). Following peptide bond formation, the tRNAs are bound in a hybrid state, and translocation to the next codon results in dissociation of one tRNA and placement of the other fully in the P-site; this opens the A-site for binding of an incoming acceptor tRNA (Moazed and Noller, 1989; Wilson and Noller, 1998). Indeed, the hybrid state of the ribosome exhibits low reactivity with puromycin, whereas there is high reactivity with puromycin following translocation (Semenkov *et al*., 1992). The behaviors of these ribosomal states are strikingly similar to those of the 80S and 80S* states reported herein. It will be of interest to determine the behaviors of the 80S and 80S* complexes when an aminoacyl-tRNA acceptor is used in place of puromycin.

There are, of course, other possibilities for the nature of this conversion step besides a conformational change in the ribosome, including the possibility of a GTP-dependent release of bound initiation factors from the 80S complex. Non-physiological origins for the observed activation must also be considered. For example, several treatments previously have been shown to result in ribosomes with low activity. Zamir, Elson and co-workers discovered a low activity state of the prokaryotic ribosome that was generated by exposure of ribosomes to low salt or Mg^{2+} concentrations (Zamir *et al*., 1974; Moazed *et al*., 1986), and Cox *et al*. (1976) reported a similar conformational state of the eukaryotic 60S ribosomal subunit that occurred upon exposure to low Mg^{2+} concentrations. These low salt/Mg^{2+}-induced transitions, however, are reversed simply by incubating the ribosomes at standard Mg^{2+} and salt concentrations at moderate temperatures, whereas the conversion of 80S to 80S* complexes does not occur in the absence of the HSW factors. A decrease in the activity of rabbit reticulocyte translation systems, apparently as the result of the pressure during ultracentrifugation, has also been reported (Henderson and Hardesty, 1978; Morley and Hershey, 1990). This inhibition was shown to result in part from activation of the hemin-controlled repressor (HCR), which is an eIF2 kinase (Henderson and Hardesty, 1978; Clemens, 1996). However, HCR is unlikely to be responsible for formation of low activity 80S complexes because HCR inhibits formation of the ternary complex, a step prior to 80S complex formation (see Figures 1 and 7). Furthermore, inclusion in the reactions of 200 μM hemin, which represses HCR (Morley and Hershey, 1990; Clemens, 1996), did not alter the kinetics of the overall reaction (data not shown). Most generally, the observed efficient inhibition of the activation process by GMP-PNP suggests the physiologically relevant action of a GTPase.

Materials and methods

Reagents

Puromycin and rabbit total tRNA were from Sigma; GTP from Pharmacia; GMP-PNP, AMP-PNP and yeast total tRNA from Boehringer Mannheim; [^{35}S]methionine from Dupont NEN; rabbit reticulocytes were from Pel-

Freez (Roders, Arkansas); Polygram IONEX-25 SA-Na cation exchange TLC plates from Alltech (Deerfield, IL); and cap analog was from New England Biolabs.

Production of model mRNA template

The model mRNA was synthesized by T7 polymerase run-off transcription of the DNA oligonucleotide template 5′-GAG AGA GAG AGA GAG AGA GAG CAT AGA GAG AGA GAG AGA TTC CTA TAG TGA GTC GTA TTA CAT ATG CGT GTT ACC-3′ (Milligan *et al*., 1987). Capped mRNA was synthesized by decreasing the concentration of GTP in the transcription from 5 to 2.5 mM and including 5 mM cap analog (7-methylGpppG; Nielsen and Shapiro, 1986). Transcripts were purified by electrophoresis on 12% polyacrylamide–8 M urea gels, eluted into 0.4 M NaCl, ethanol precipitated and resuspended in water.

Preparation of ribosomes and HSW

Rabbit reticulocyte lysate was prepared and treated with micrococcal nuclease as described previously (Crystal *et al*., 1974; Pelham and Jackson, 1976). The ribosome and HSW preparation procedure was adapted from previous protocols (Crystal *et al*., 1974; Merrick, 1979). Crude ribosomes from 3 ml of lysate were pelleted in 13 × 51 mm polycarbonate tubes in a Beckman TL100.3 rotor at 65 000 r.p.m. for 2 h. The supernatant was discarded and the ribosome pellet was dissolved in 1 ml of buffer A [30 mM HEPES–KOH pH 7.4, 100 mM potassium acetate, 2 mM magnesium acetate, 0.1 mM EDTA, 2 mM dithiothreitol (DTT)] plus 0.4 M potassium chloride and 0.25 M sucrose at 0°C. The ribosome solution was layered onto 2 ml of buffer A plus 0.4 M potassium chloride and 1 M sucrose and centrifuged at 85 000 r.p.m. for 2 h as described above. The supernatant (HSW) was dialyzed against 1 l of buffer A plus 10% glycerol overnight, after which aliquots were flash-frozen in liquid N_2 and stored at –80°C. The ribosomal pellet was dissolved in buffer A plus 0.25 M sucrose. Aliquots were frozen and stored as for the HSW. Ribosome concentrations were measured using an extinction coefficient of $\varepsilon_{260} = 5 \times 10^7$/M/cm (Matasova *et al*., 1991).

tRNA charging

Yeast methionyl-tRNA$_i$ in yeast total tRNA was charged with [^{35}S]methionine using a crude preparation of *Escherichia coli* tRNA sythetases (Stanley, 1974; Merrick, 1979). After charging, the reactions were extracted with phenol, then with chlorofrom, ethanol precipitated at pH 4.6, and resuspended in water. The concentration of Met-tRNA$_i$ was calculated based on the known specific activity of the [^{35}S]methionine. Rabbit total tRNA (Sigma) was also tested but was found to produce a high background of non-specific binding of ^{35}S-labeled material to the TLC plates. Nevertheless, the 80S to 80S* transition described in the Results was also observed with rabbit Met-tRNA$_i$, indicating that this transition is not specific to yeast tRNA$_i$ (data not shown). A preparation of yeast [^{35}S]Met-tRNA$_i$ that was partially purified by reverse phase HPLC after charging gave the same kinetics in the overall puromycin assay as the unpurified material (data not shown).

Puromycin assay

Standard assay buffer conditions were 32 mM HEPES–KOH pH 7.4, 140 mM potassium acetate, 3.3 mM magnesium acetate, 2.8 mM DTT and 4% glycerol, which includes contributions from the ribosomes and HSW. The concentrations of components in a standard reaction are given in Table I. All reactions were performed at 26°C. The rate constants for the two slow steps increase ~2-fold when the temperature is increased to 37°C (not shown). The lower temperature was used for consistency with previous work using rabbit reticulocyte lysate, to prevent problems from evaporation, and because the system loses activity quickly at higher temperature (data not shown). Standard reaction volumes were 10–25 µl. Unless otherwise noted, reactions were initiated by the addition of 10× puromycin. Aliquots (2 µl) from the reaction were withdrawn at various times and quenched in 0.5 µl of 3 M sodium acetate pH 4.6. Potassium hydroxide (0.5 M) or 1% SDS were also effective quenches, although KOH hydrolyzes the ester linkage between the tRNA and methionine (see Figure 2). Samples were spotted onto Polygram IONEX-25 SA-Na cation exchange TLC plates (6.5 × 20 cm). The plates were air dried and developed in 2 M ammonium acetate pH 5.2 plus 10% acetonitrile. Dried plates were exposed overnight on a PhosphorImager screen and analyzed and quantitated using the PhosphorImager (Molecular Dynamics). The PhosphorImager detection allows ~50 time points to be exposed overnight per PhosphorImager plate, which greatly increases the sensitivity of the assay relative to scintillation counting in which overnight exposures of individual time points would be prohibitively time consuming. Spots corresponding to [^{35}S]Met-tRNA$_i$ and free methionine were identified by standards. Identification of the Met–Puro spot was made by ethyl acetate extraction of a standard puromycin reaction and running this ethyl acetate-soluble material (Met–Puro) alone and added to a reaction mix (Leder and Bursztyn, 1966; Merrick, 1979; data not shown). As expected, appearance of the Met–Puro spot depended on the presence of ribosomes, HSW, GTP and puromycin in the reactions. The presence of saturating mRNA stimulates Met–Puro formation ~10-fold; the background is probably due to endogenous mRNA fragments in the ribosome and HSW preparations. No stimulation over background was observed with a model mRNA lacking an AUG codon at concentrations from 0.3 to 10 µM. Similar results for the kinetics of the overall reaction were obtained using the TLC method and the ethyl acetate extraction method (data not shown).

Native gel assay

Standard reaction conditions and concentrations were the same as for the puromycin assay. Native gel buffer (THEM) was 66 mM HEPES acid, 34 mM Tris base, 2.5 mM $MgCl_2$, 0.1 mM EDTA (final pH 7.5). Native gels were 4% acrylamide (37.5:1 acrylamide:bisacrylamide) in THEM. The gel temperature was maintained at ~26°C by cooling. The typical reaction volume was 70 µl. Aliquots (10 µl) were withdrawn at various times and mixed with 1 µl of 50% sucrose, 0.02% each bromophenol blue and xylene cyanol, and then immediately loaded onto a running gel. The sucrose solution prevents extensive mixing of the sample with the running buffer prior to running into the gel. Loading powers from 8 to 24 W had no effect on the results (data not shown), suggesting that the complexes migrate into the gel on a time scale faster than 43S or 80S complex formation or dissociation occurs. Gels were dried on Whatman paper and exposed overnight on a PhosphorImager screen. A sample of each reaction mix was spotted onto the filter paper prior to exposure to allow the actual amount of product formed to be calculated (see next section). Identification of the complexes was made based on the following observations: (i) only the 43S·mRNA complex band accumulates in the presence of GMP-PNP; (ii) only the 43S complex band accumulates in the presence of 10 µM edeine, a drug that blocks the 60S subunits joining step (data not shown; Santon and Stanley, 1978); (iii) formation of the 80S complex band requires the presence of GTP; (iv) formation of both bands requires the presence of ribosomes and HSW; (v) the complexes contain both mRNA and Met-tRNA$_i$, as shown in Figure 3; and (vi) the bands migrate similarly to the positions reported by Dahlberg (1979) for prokaryotic ribosomal complexes using a similar native gel system. Composite gels (3% acylamide/0.5% agarose) were also tested. Although comparable bands were observed, it was found that 4% acrylamide gave sharper bands.

The material at the top of the gels (Figure 3) may be RNA–protein aggregates as its presence depends on the presence of HSW but not ribosomes (data not shown). With [^{35}S]Met-tRNA$_i$, this slow migrating material is 5–10% of the input tRNA, and <20% the amount of the 43S or 80S complexes formed. This material does not increase significantly on the time scale of the experiments. Although the amount of this material in the ^{32}P-labeled mRNA experiment is similar to the amount of 43S or 80S complexes, this slow migrating material and the 43S/80S complexes are each ≤5% of the input mRNA so that the formation of the slow migrating material does not significantly affect the concentration of free mRNA in the assays.

General kinetics

Except where noted, time courses of reaction were followed for >4 half-lives. In the puromycin assays, the fraction of [^{35}S]Met-tRNA at the start of the reaction converted to Met–Puro at each time point was calculated. In the native gel assays, the fraction of [^{35}S]methionine in the reaction converted to the product (43S·mRNA or 80S) was calculated and no correction was made for the small amount (<10%) of free methionine present at the start of the reaction. Hydrolysis of [^{35}S]Met-tRNA to give free methionine was followed using the TLC assay and found to be ≤10% over the course of a standard assay (15 min). Data were fit by one of three equations. For the overall reaction, a fit of an equation describing a simple two-step process was used (Equation 1; Fersht, 1985), in which A is the amplitude and k_1 and k_2 are the observed rate constants for step 1 and step 2, respectively.

$$\text{Fraction product} = A\left(1 + \frac{1}{k_1 - k_2}\left[k_2 \exp(-k_1 t) - k_1 \exp(-k_2 t)\right]\right) \quad (1)$$

The observed rate constants from these fits were assigned to individual processes because pulse–chase experiments suggested that the formation

of the ribosomal complexes was essentially irreversible (data not shown). When the reaction had only a single slow step, the data were fit by a single first-order exponential equation (Fersht, 1985). For cases in which part of the ribosomes were 80S complexes and part were the more reactive 80S* complexes, the data were fit by a double exponential equation (Equation 2; Fersht, 1985), in which A_1 and A_2 are the amplitudes of the two phases and k_1 and k_2 are the rate constants.

$$\text{Fraction product} = A_1[1 - \exp(-k_1 t)] + A_2[1 - \exp(-k_2 t)] \quad (2)$$

All fits were performed using KaleidaGraph software (Synergy Software). In all cases, observed first-order rate constants (k_{obs}) for the step in question under the conditions of this assay system are given. This does not imply that the step is necessarily first-order, and in no case are these rate constants known to be fundamental rate constants for the step.

End points of the standard puromycin reactions varied from 0.15 to 0.2 (fraction of Met–Puro formed relative to the input [^{35}S]Met-tRNA). Several factors may cause this value to be <1. Some of the [^{35}S]Met-tRNA may be unreactive or inaccessible for reaction at the start of the reaction or may become unreactive during the assay. For example, the *E.coli* tRNA synthetases can also charge the yeast elongator methionyl-tRNA to some extent, so a fraction of the labeled tRNA may not have been initiator tRNA and thus could not take part in initiation (Stanley, 1974). In addition, some of the initiator tRNA may form non-productive complexes with RNA-binding proteins present in the system, and ~10% of the ester linkages between the amino acid and tRNA are hydrolyzed during the standard reaction (see above). Finally, other competing processes such as inactivation of ribosomes and initiation factors may contribute to the lower than stoichiometric conversion of the input [^{35}S]Met-tRNA$_i$.

The following lines of evidence suggest that reactions are single turnover, i.e. that ribosomes are not recycled to allow formation of a second molecule of [^{35}S]Met–Puro from a second [^{35}S]Met-tRNA$_i$. First, the data suggest that the concentration of active ribosomes is in excess of [^{35}S]Met-tRNA$_i$ (Table I). Secondly, the reactions from 80S and 80S* complexes are not significantly inhibited by the addition of poly(U) or unlabeled Met-tRNA$_i$ or by a 5-fold dilution, all of which significantly inhibit the reactions if added or performed at step 1 (Figure 1; data not shown). If a small amount of active ribosomal subunits were recycling multiple times during the course of the reaction, these inhibitors of initiation would be expected to slow the reactions when added in the midst of a time course as well as at the beginning.

The puromycin reaction was used to determine suitable standard conditions (Table I). To accomplish this, apparent Michaelis constants for the components of the reaction were determined (Table I). Values are apparent K_ms because the reactions are single turnover whereas the standard Michaelis constant is defined for multiple turnover conditions in which [enzyme]<<[substrate] (Fersht, 1985). To measure reactions starting with the 80S complex, the HSW, Met-tRNA$_i$ and GTP were pre-incubated for 5–10 min to allow the first slow step to be passed (step 1, Figure 1; see 'Is the formation of the ternary complex or the 43S·mRNA complex the first slow step?' in Results). The reactions were then initiated with ribosomes and puromycin. To start reactions at 80S*, the components were pre-incubated for 10 min and the reaction was then initiated with puromycin, as described in 'Activation of the 80S complex' in Results. Concentrations of substrates from at least 3-fold below the apparent K_m to at least 4-fold above it were used. Nucleotides were always added as the stoichiometric complex with Mg^{2+}. As the concentrations of substrates are lowered, the end points of the reactions decrease (maximally by 4-fold), presumably because the rate of reaction slows relative to the rates of competing processes such as inactivation of factors or ribosomes. The measured k_{obs} values were corrected for these changing end points by assuming an end point identical to that obtained with saturating substrate, i.e. k_{obs} was multiplied by the observed end point and divided by that with saturating substrate. In all cases, initial rates were also measured, and the K_m values determined in this way were in good agreement with those determined using corrected k_{obs} values. The k_{obs} or initial velocity versus [substrate] data were fit by the Michaelis–Menten equation to determine the apparent K_m (Fersht, 1985). *R*-values for the fits of all plots were ≥0.96.

The observed rate constants for the reaction subsequent to the lag increase linearly with the concentration of ribosomes up to ~60 nM, at which point they begin to decrease (data not shown), presumably due to the presence of an inhibitor in the ribosome preparations. The observed rate constants for both phases of the reaction are constant from 0.5 to 10 nM Met-tRNA$_i$ with 60 nM ribosomes. These data are consistent with a system in which active ribosomes are in excess of Met-tRNA$_i$.

GMP-PNP inhibition

GMP-PNP inhibition experiments were performed in a background of 100 μM GTP, except where noted. The apparent K_i for GMP-PNP was determined by measuring the k_{obs} for reaction from the pre-formed 80S complex as a function of [GMP-PNP] (1–1000 μM). Data were fit by the equation for competitive inhibition (Fersht, 1985). It was shown in a separate experiment that inhibition by GMP-PNP could be overcome by adding sufficient GTP, suggesting that the inhibition is competitive (data not shown).

Measurement of fast kinetics

To measure small extents of reaction from the 80S* complex, each 5 μl reaction was initiated with 10× puromycin and then quenched by adding 1.3 μl of 3 M sodium acetate pH 4.6 at the appropriate time. By having the quench solution already loaded in a pipet directly above the reaction mixture when the reactions are initiated, accurate time points as short as 5 s could be taken. Time points were analyzed as described above.

Estimation of errors

Rate constants measured in the same experiment differed by no more than 50%, whereas rate constants measured on different days occasionally varied by as much as 2-fold. To give a sense of the errors of the measurements, ranges of values from independent experiments are given in the text and figure legends.

Acknowledgements

We are grateful to Alan Sachs, Peter Sarnow, John Hershey and members of our laboratory for critical reading of this manuscript. We thank Alan Sachs and Rachel Green for advice and discussions. J.R.L. gratefully acknowledges a Leukemia Society of America Special Fellowship. This work was supported by a David and Lucile Packard Foundation Fellowship in Science and Engineering to D.H.

References

Abel,K. and Jurnak,F. (1996) A complex profile of protein elongation: translating chemical energy into molecular movement. *Structure*, **4**, 229–238.

Anthony,D.D. and Merrick,W.C. (1992) Analysis of 40S and 80S complexes with mRNA as measured by sucrose density gradients and primer extension inhibition. *J. Biol. Chem.*, **267**, 1554–1562.

Benkovic,S.J. and Cameron,C.E. (1995) Kinetic analysis of nucleotide incorporation and misincorporation by Klenow fragment of *Escherichia coli* DNA polymerase I. *Methods Enzymol.*, **262**, 257–269.

Benne,R. and Hershey,J.W.B. (1979) The mechanism of action of protein synthesis initiation factors from rabbit reticulocytes. *J. Biol. Chem.*, **253**, 3078–3087.

Chatterjee,B., Dasgupta,A., Majumdar,A., Palmieri,S. and Gupta,N.K. (1979) Millipore filtration assay for AUG-directed Met-tRNA binding to 40S and 80S ribosomes. *Methods Enzymol.*, **60**, 256–265.

Cheng,S.C. and Abelson,J. (1987) Spliceosomal assembly in yeast. *Genes Dev.*, **1**, 1014–1027.

Clemens,M.J. (1996) Protein kinases that phosphorylate eIF2 and eIF2B and their role in eukaryotic cell translational control. In Hershey,J.W.B., Matthews,M.B. and Sonenberg,N. (eds), *Translational Control*. Cold Spring Harbor Laboratory Press, Cold Spring Harbor, NY, pp. 139–172.

Cox,R.A., Greenwell,P. and Hirst,W. (1976) Re-activation of the peptidyltransferase centre of rabbit reticulocyte ribosomes after exposure to low concentrations of magnesium ion. *Biochem. J.*, **160**, 521–531.

Crystal,R.G., Elson,N.A. and Anderson,W.F. (1974) Initiation of globin synthesis assays. *Methods Enzymol.*, **30**, 101–127.

Dahlberg,A.E. (1979) A gel electrophoretic separation of bacterial ribosomal subunits with and without protein S1. *Methods Enzymol.*, **1979**, 397–401.

Das,H.K., Das,A., Ghosh-Dastidar,P., Ralston,R.O., Yaghami,B., Roy,R. and Gupta,N.K. (1981) Protein synthesis in rabbit reticulocytes. Purification and characterization of a double-stranded RNA-dependent protein synthesis inhibitor from reticulocyte lysates. *J. Biol. Chem.*, **256**, 6491–6495.

Fersht,A. (1985) *Enzyme Structure and Mechanism*. W.H.Freeman and Co., New York.

Gilbert,S.P., Webb,M.R., Brune,M. and Johnson,K.A. (1995) Pathway of processive ATP hydrolysis by kinesin. *Nature*, **373**, 671–676.

Hawley,D.K. and Roeder,R.G. (1985) Separation and partial

characterization of three functional steps in transcription initiation by human RNA polymerase II. *J. Biol. Chem.*, **260**, 8163–8172.
Henderson,A.B. and Hardesty,B. (1978) Evidence for an inhibitor of protein synthesis in rabbit reticulocytes activated by high pressure. *Biochem. Biophys. Res. Commun.*, **83**, 715–723.
Jackson,R.J. (1996) A comparative view of initiation site selection mechanisms. In Hershey,J.W.B., Mathews,M.B. and Sonenberg,N. (eds), *Translational Control*. Cold Spring Harbor Laboratory Press, Cold Spring Harbor, NY, pp. 71–112.
Jencks,W.P. (1987) *Catalysis in Chemistry and Enzymology.* Dover, New York, NY.
Johnson,F.B. and Krasnow,M.A. (1992) Differential regulation of transcription preinitiation complex assembly by activator and repressor homeo domain proteins. *Genes Dev.*, **6**, 2177–2189.
Kadonaga,J.T. (1990) Assembly and disassembly of the *Drosophila* RNA polymerase II complex during transcription. *J. Biol. Chem.*, **265**, 2624–2631.
Konarska,M.M. and Sharp,P.A. (1986) Electrophoretic separation of complexes involved in the splicing of precursors to mRNAs. *Cell*, **46**, 845–855.
Leder,P. and Bursztyn,H. (1966) Initiation of protein synthesis II. A convenient assay for the ribosome-dependent synthesis of *N*-formyl-^{14}C-methionylpuromycin. *Biochem. Biophys. Res. Commun.*, **25**, 233–238.
Marcotrigiano,J., Gingras,A.C., Sonenberg,N. and Burley,S.K. (1997) Cocrystal structure of the messenger RNA 5′ cap-binding protein (eIF4E) bound to 7-methyl-GDP. *Cell*, **89**, 951–961.
Matasova,N.B., Myltseva,S.V., Zenkova,M.A., Graifer,D.M., Vladimirov,S.N. and Karpova,G.G. (1991) Isolation of ribosomal subunits containing intact rRNA from human placenta: estimation of functional activity of 80S ribosomes. *Anal. Biochem.*, **198**, 219–223.
Matsuo,H., McGuire,A.M., Fletcher,C.M., Gingras,A.C., Sonenberg,N. and Wagner,G. (1997) Structure of translation factor eIF4E bound to m7GDP and interaction with 4E-binding protein. *Nature Struct. Biol.*, **4**, 717–724.
McCarthy,J.E.G. (1998) Posttranscriptional control of gene expression in yeast. *Microbiol. Mol. Biol. Rev.*, **62**, 1492–1553.
Merrick,W.C. (1979) Assays for eukaryotic protein synthesis. *Methods Enzymol.*, **60**, 108–123.
Merrick,W.C. and Hershey,J.W.B. (1996) The pathway and mechanism of eukaryotic protein synthesis. In Hershey,J.W.B., Mathews,M.B. and Sonenberg,N. (eds), *Translational Control*. Cold Spring Harbor Laboratory Press, Cold Spring Harbor, NY, pp. 31–69.
Milligan,J.F., Groebe,D.R., Witherell,G.W. and Uhlenbeck,O.C. (1987) Oligoribonucleotide synthesis using T7 RNA polymerase and synthetic DNA templates. *Nucleic Acids Res.*, **15**, 8783–8798.
Moazed,D. and Noller,H.F. (1989) Intermediate states in the movement of transfer RNA in the ribosome. *Nature*, **342**, 142–148.
Moazed,D., VanStolk,B.J., Douthwaite,S. and Noller,H.F. (1986) Interconversion of active and inactive 30S ribosomal subunits is accompanied by a conformational change in the decoding region of 16S rRNA. *J. Mol. Biol.*, **191**, 483–493.
Morley,S.J. and Hershey,J.W.B. (1990) A fractionated reticulocyte lysate retains high efficiency for protein synthesis. *Biochimie*, **72**, 259–264.
Nesset,C.C. and Dickman,S.R. (1980) Effects of potassium chloride concentration on protein content and polyphenylalanine synthesizing capability of 40S ribosomal subunits from canine pancreas. *Biochemistry*, **19**, 2731–2737.
Nielsen,D.A and Shapiro,D.J. (1986) Preparation of capped RNA transcripts using T7 RNA polymerase. *Nucleic Acids Res.*, **14**, 5936.
Nissen,P., Kjeldgaard,M., Thirup,S., Clark,B.F. and Nyborg,J. (1996) The ternary complex of aminoacylated tRNA and EF-Tu-GTP. Recognition of a bond and a fold. *Biochimie*, **78**, 921–933.
Palmiter,R.D. (1975) Quantitation of parameters that determine the rate of ovalbumin synthesis. *Cell*, **4**, 189–197.
Pape,T., Wintermeyer,W. and Rodnina,M.V. (1998) Complete kinetic mechanism of elongation factor Tu-dependent binding of aminoacyl-tRNA to the A site of the *E.coli* ribosome. *EMBO J.*, **17**, 7490–7497.
Pelham,H.R.B. and Jackson,R.J. (1976) An efficient mRNA-dependent translation system from reticulocyte lysates. *Eur. J. Biochem.*, **67**, 247–256.
Pestova,T.V. and Hellen,C.U.T. (1999) Ribosome recruitment and scanning: what's new? *Trends Biochem. Sci.*, **24**, 85–87.
Pestova,T.V., Borukhov,S.I. and Hellen,C.U.T. (1998) Eukaryotic ribosomes require initiation factors 1 and 1A to locate initiation codons. *Nature*, **394**, 854–859.
Pollard,T.D. (1986) Assembly and dynamics of the actin filament system in nonmuscle cells. *J. Cell Biochem.*, **31**, 87–95.
Rodnina,M.V., Savelsbergh,A., Katunin,V.I. and Wintermeyer,W. (1997) Hydrolysis of GTP by elongation factor G drives tRNA movement on the ribosome. *Nature*, **385**, 37–41.
Saenger,W. (1984) *Principles of Nucleic Acid Structure*. Springer-Verlag, New York, NY.
Santon,J.B. and Stanley,W.M. (1978) Stability of protein synthesis initiation complexes in the presence of edeine. *Biochem. Biophys. Res. Commun.*, **84**, 985–992.
Semenkov,Y.P., Shapkina,T.G. and Kirillov,S.V. (1992) Puromycin reaction of the A-site bound peptidyl-tRNA. *Biochimie*, **74**, 411–417.
Seraphin,B. and Rosbash,M. (1989) Identification of functional U1 snRNA–pre-mRNA complexes committed to spliceosomal assembly and splicing. *Cell*, **59**, 349–358.
Stanley,W.M.J. (1974) Specific aminoacylation of the methionine-specific tRNAs of eukaryotes. *Methods Enzymol.*, **29**, 530–547.
Stryer,L. (1986) Cyclic GMP cascade of vision. *Annu. Rev. Neurosci.*, **9**, 87–119.
Svitkin,Y.V., Ovchinnikov,L.P., Dreyfuss,G. and Sonenberg,N. (1996) General RNA binding proteins render translation cap dependent. *EMBO J.*, **15**, 7147–7155.
Tarun,S.Z. and Sachs,A.B. (1995) A common function for mRNA 5′ and 3′ ends in translation initiation in yeast. *Genes Dev.*, **9**, 2997–3007.
Trachsel,H. (1996) Binding of initiator methionyl-tRNA to ribosomes. In Hershey,J.W.B., Matthews,M.B. and Sonenberg,N. (eds), *Translational Control*. Cold Spring Harbor Laboratory Press, Cold Spring Harbor, NY, pp. 113–138.
Trachsel,H., Erni,B., Schreier,M.H. and Staehelin,T. (1977) Initiation of mammalian protein synthesis. II. The assembly of the initiation complex with purified initiation factors. *J. Mol. Biol.*, **116**, 755–767.
Vossen,K.M. and Fried,M.G. (1997) Sequestration stabilizes lac repressor–DNA complexes during gel electrophoresis. *Anal. Biochem.*, **245**, 85–92.
Wieczorek,Z., Darzynkiewicz,E. and Lonnberg,H. (1998) A fluorescence spectroscopic study on the binding of mRNA 5′-cap-analogs to human translation initiation factor eIF4E: a critical evaluation of the sources of error. *J. Photochem. Photobiol.*, **B43**, 158–163.
Wilson,K.S. and Noller,H.F. (1998) Molecular movement inside the translational engine. *Cell*, **92**, 337–349.
Yount,R.G. (1975) ATP analogs. *Adv. Enzymol. Rel. Areas Mol. Biol.*, **43**, 1–56.
Zamir,A., Miskin,R., Vogel,Z. and Elson,D. (1974) The inactivation and reactivation of *Escherichia coli* ribosomes. *Methods Enzymol.*, **30**, 406–426.

Received July 26, 1999; revised and accepted October 8, 1999